Energy & Environmental Science

ANALYSIS

Climate change impacts on future photovoltaic and concentrated solar power energy output

Julia A. Crook,[a] Laura A. Jones,[b] Piers M. Forster[a] and Rolf Crook[*b]

Building large solar power plants requires significant long-term investment so understanding impacts from climate change will aid financial planning, technology selection, and energy output projections. In this article we examine how projected changes in temperature and insolation over the 21st century will affect photovoltaic (PV) and concentrated solar power (CSP) output. Projected climate data was obtained from the coupled ocean-atmosphere climate models HadGEM1 and HadCM3 under the IPCC SRES A1B scenario which describes a future world of rapid economic growth with a balanced use of renewable and fossil fuel power generation. Our calculations indicate that under this scenario PV output from 2010 to 2080 is likely to increase by a few percent in Europe and China, see little change in Algeria and Australia, and decrease by a few percent in western USA and Saudi Arabia. CSP output is likely to increase by more than 10% in Europe, increase by several percent in China and a few percent in Algeria and Australia, and decrease by a few percent in western USA and Saudi Arabia. The results are robust to uncertainty in projected temperature change. A qualitative analysis of uncertainty in projected insolation change suggests strongest confidence in the results for Europe and least confidence in the results for western USA. Changes in PV and CSP output are further studied by calculating fractional contributions from changes in temperature and insolation. For PV there is considerable variation in contribution depending on location. For CSP the contribution from changes in insolation is always dominant.

Introduction

Within the next 100 years it is widely accepted that the Earth's climate will see notable change because of the anthropogenic emission of greenhouse gases and aerosols. Current and future solar power plants with MW and GW generation capacity represent a considerable investment in plant, infrastructure, and land, so understanding likely impacts from climate change will assist site choice, critical long-term energy output and financial calculations. While solar technology is likely to be upgraded or replaced well within this 100 year timescale, there is often a strong economic and environmental case to continue using existing sites.

[a]Institute for Climate and Atmospheric Science, School of Earth and Environment, University of Leeds, LS2 9JT, UK. E-mail: R.Crook@leeds.ac.uk; Fax: +44 (0)113 246 7310; Tel: +44 (0)113 246 7310
[b]Energy and Resources Research Institute, School of Process, Environmental and Materials Engineering, University of Leeds, LS2 9JT, UK

Broader context

Massive solar power plants are likely to make a significant contribution to electricity generation in our low-carbon future. However, this future will also experience significant climate change caused by past and ongoing emissions of greenhouse gases and aerosols. This work calculates how climate change is likely to alter the output of photovoltaic and concentrated solar power plants over the next 80 years, taking a global perspective. Established computer models, that include a sophisticated picture of cloud properties and aerosols, indicate that change in solar power plant output will show considerable regional differences. For example, output is likely to increase significantly in Europe, but decrease in many parts of the world such as western America and the Middle East. This is caused by either change in temperature or insolation, again with considerable regional differences. Climate change will have a notable impact on plant output, so planners, policy makers, and investors of solar energy must include climate change in their longer term projections. This work, and future regional studies, will enable more informed decisions regarding the location, type of technology, projected power output, and rate of return, for large solar power plants.

PV and CSP are the two most widely installed solar technologies for large-scale electricity generation. PV cells directly convert sunlight into electricity using a semiconductor junction. The cells can be manufactured from a variety of semiconductor materials, but monocrystalline and multicrystalline silicon cells lead the mass-production market.[1] Calculations are performed for non-concentrating grid-connected monocrystalline silicon PV. Other PV technologies are briefly considered at the end of this article. CSP is an indirect method of converting sunlight into electricity. Sunlight is focussed by collector mirrors or lenses onto an absorber. A heat transfer fluid continually circulates through pipes embedded in the absorber, which raises steam to drive a turbine-generator set. A variety of CSP technologies have been demonstrated, including parabolic troughs, solar power towers, concentrating Fresnel lenses, and Stirling solar dishes.[2] The parabolic trough is the most common and established of these technologies, and is considered here.

PV output has a near linear response to cell temperature with a negative gradient, and an approximately proportional response to total irradiance except under low levels. CSP output has an approximately linear response to ambient temperature with a positive gradient, and an approximately proportional response to direct irradiance. CSP does not utilise diffuse irradiance whereas non-concentrating PV utilises both direct and diffuse irradiance. Irradiance is largely a function of cloud cover and cloud properties. Climate change will impact regional patterns of temperature and irradiance, and therefore affect regional PV and CSP output. Our research projects the impact of climate change on the energy output of both technologies globally and in selected regions over the 21st century.

Solar power plants are and will continue to be located close to centres of population within the Earth's sun belt of 40°N to 40°S on account of the higher insolation (time average surface irradiance). Most operational plants are clustered in the USA and Europe, while numerous new plants are planned or under construction worldwide. Outside the sun belt, in locations such as Germany, PV plants are preferred over CSP because lower levels of direct insolation make CSP less economically attractive.

Method

Climate models and scenario

Climate data was obtained for two respected climate models, HadGEM1[3] and HadCM3,[4] from the World Climate Research Programme's (WCRP's) Coupled Model Intercomparison Project phase 3 (CMIP3) multi-model dataset. It must be noted that modelled projections of regional temperature and especially cloud changes, and therefore insolation, have large uncertainties.[5] Models are assessed by considering how accurately they reproduce past climate. Our own analysis of 1980–1990 mean surface temperature (climatology) in HadCM3 and HadGEM1 (20c3m experiments) suggest that in the regions of interest for solar power the models are within −6 °C to 1 °C of ERA40[6] observations in all months. HadCM3 was found to be one of the best performing models for annual global mean clear-sky insolation in a study of 14 CMIP3 models not including HadGEM1.[7] This study also showed that reproduction of clear-sky insolation

has improved in the CMIP3 models compared to the previous generation models. Bodas-Salcedo et al.[8] assessed the radiation budget of the HadGEM1 model forced with observed sea surface temperatures and found insolation tended to be overestimated compared to the International Satellite Cloud Climatology Project (ISCCP) fluxes by the model over land particularly in the summer. Our own comparisons of the modelled current 1980–1999 mean insolation compared to that obtained from the Edwards-Slingo radiative transfer model[9] using current climatology based on ISCCP clouds, suggests both models underestimate insolation in Europe and China by up to 80 W m^{-2} in some months, and in other regions of interest the models are mostly within ± 40 W m^{-2}. HadGEM1 was found to be slightly better than HadCM3 and may be more reliable at reproducing future changes because it includes a more physical realisation of aerosols.

The data from the models forced with IPCC emissions scenario SRES A1B[10] was used to assess future climate change. This scenario describes a future world of very rapid economic growth, global population that peaks in mid-century and declines thereafter, and the rapid introduction of new and more efficient technologies with a balanced use of renewable and fossil fuel power generation. Anthropogenic emissions of greenhouses gases and sulphate aerosols were specified, but other species such as tropospheric and stratospheric ozone, all of the non-sulphate aerosols, and the indirect effects of aerosols on cloud albedo and lifetime were left to the discretion of the different modelling groups. The best-estimate of global temperature rise by 2100 relative to the 1980–1999 mean for this scenario is 2.8 °C (1.7 °C to 4.4 °C all model range, 3.0 °C for HadCM3, 3.4 °C for HadGEM1). This realistic scenario is consistent with the installation of large PV and CSP plants implicit of this work.

The climate model data obtained consists of monthly means of near surface temperature (T), fractional cloud cover (C_f), total insolation for the actual cloud cover (G_{tot}), and clear-sky total insolation for if there were no clouds present (G_{cs}). For concentrating technologies, direct insolation is required. Using annual global means of the output from the Edwards-Slingo radiative transfer model,[9] we found the empirical relationship between the direct insolation (G_{dir}) and G_{cs} was

$$G_{dir} = 0.75 G_{cs}(1 - C_f). \tag{1}$$

The factor 0.75 is required because scattering of sunlight by air molecules and aerosols occurs even under clear-sky conditions. The climate data are means over day and night but only daytime temperatures and insolation are required in this work. To adjust to daytime monthly mean temperature (T_{day}), it was assumed that the temperature varies roughly sinusoidally over the day with an amplitude of $DTR/2$, where DTR is the diurnal temperature range (temperature difference between maximum and minimum daily temperatures), and a mean value of T, so that T_{day} can be approximated as

$$T_{day} = \overline{T} + \frac{\overline{DTR}}{4} \tag{2}$$

where overbar indicates monthly means. Minimum and maximum temperatures are not available for our chosen models. Therefore the current climatological DTR for each month from

the HadCRUT3 temperature dataset[11] was used and we assumed that DTR did not change in future. In fact, there is no clear consensus on whether DTR will change in future.[12] The average insolation over the daylight hours when the technology is working was estimated by scaling the insolation by the day length,

$$G_{day} = \overline{G} \frac{t_{24h}}{t_{daylength}} \qquad (3)$$

where $\bar{G}$ is the monthly mean of G_{tot} when considering PV or G_{dir} when considering CSP. The day length is used again to scale the average power output for each month when calculating the energy output for each month.

PV and CSP energy output equations

General equations are required for both technologies to calculate the power output as a function of irradiance and ambient temperature (previously called near surface temperature). The equations are purposely generic and inefficiencies that are independent of temperature and insolation are not included. While system specific refinements are possible, they are unlikely to cause significant differences to the results and conclusions.

The maximum power output of a PV cell is equal to the product of the fill factor (FF), the open circuit voltage (V_{oc}), and the closed circuit current (I_{cc}). Using the one-diode model for a PV cell,[13] it can be shown that the product of FF and V_{OC} responds linearly with a negative gradient to a change in cell temperature caused by thermally generated carriers. To a lesser extent, I_{cc} increases with increasing temperature. The established negative gradient linear relationship for the efficiency of a PV cell as a function of cell temperature is

$$\frac{\eta_{cell}}{\eta_{ref}} = 1 - \beta\left(T_{cell} - T_{ref}\right) + \gamma \log_{10} G_{tot} \qquad (4)$$

where η_{ref} is the reference efficiency, β and γ are respectively the temperature and irradiance coefficients set by the cell material and structure, and T_{cell} and T_{ref} are respectively the cell and reference temperatures.[14–16] Silicon PV efficiency decreases at low-light levels and this is accommodated through γ.[14] The calculations presented in this article use $\beta = 0.0045$ and $\gamma = 0.1$, which is typical for monocrystalline silicon cells, and $T_{ref} = 25\,°C$.

Following work of several authors, a general empirical expression for the cell temperature is

$$T_{cell} = c_1 + c_2 T + c_3 G_{tot} \qquad (5)$$

where T is the ambient temperature in $°C$.[17–19] The coefficients depend on details of the module and mounting that affect heat transfer from the cell. Coefficients used for the calculations are taken from Lasiner and Ang for a monocrystalline silicon cell:[19] $c_1 = -3.75\,°C$, $c_2 = 1.14$, $c_3 = 0.0175\,°C\,m^2\,W^{-1}$.

The thermal efficiency of the parabolic trough CSP system is set by collector inefficiencies and heat loss from the absorber. Following the method of Kalogirou,[2] the heat flow in to the absorber can be written to the first order as

$$q = F_R[A_c G_{dir} \eta_o - A_a c(T_i - T)] \qquad (6)$$

where F_R is the heat removal factor which is independent of T and G_{dir}, η_o is the collector optical efficiency, A_c and A_a are the areas of respectively the collector and absorber, c is a generalised heat transfer coefficient, and T_i is the temperature of the fluid entering the absorber.

The thermal efficiency of a CSP system is found by dividing q by $A_c G_{dir}$ giving

$$\eta_{csp} = F_R \eta_o - \frac{c(T_i - T)}{CG_{dir}} = k_0 - \frac{k_1(T_i - T)}{G_{dir}} \qquad (7)$$

where C is the solar concentration ratio which is equal to A_c/A_a. It is always the case that $T_i > T$, so the efficiency will increase when the ambient temperature or the direct irradiance increase. By assuming the temperature of the fluid leaving the absorber is kept constant by controlling the fluid flow rate, the efficiency of the entire plant will be approximately proportional to η_{csp}. Coefficients used in the calculations are for an Industrial Solar Technology parabolic trough collector tested at Sandia National Laboratories:[20,21] $k_0 = 0.762$, $k_1 = 0.2125\,Wm^{-2}\,°C^{-1}$, $T_i = 115\,°C$.

Equations used to calculate the power output of PV and CSP are respectively

$$P_{PV} = G_{tot}\eta_{cell} \text{ and } P_{CSP} = G_{dir}\eta_{CSP} \qquad (8)$$

The value of η_{ref} is not important, because only the fractional change in power output, $\Delta P/P$, is considered. The calculations of monthly mean P_{PV} and P_{CSP} used T_{day} and G_{day}. Small errors will arise from non-linear terms of G and T in eqn (4) and (7) because the variation of G and T throughout the day is time averaged. A numerical simulation under clear-sky conditions suggests the errors amount to 1% to 2% depending on latitude. However, these errors are highly systematic and have little effect on the percentage change in energy output from year-to-year. Annual energy output is given by

$$E = \sum_{month} 30 P t_{daylength} \qquad (9)$$

assuming 30 days for each month.

Regions studied

Several regions were selected for study, on account of existing or planned large PV or CSP solar power plants. These regions are shown on the global map of Fig. 1 (a) and listed in Table 1 which also identifies the PV and CSP plants. Desertec (EU-MENA) is an ambitious plan to integrate PV and CSP plants to provide approximately half of the electricity used by Europe, the Middle East, and northern Africa by 2050.[22] A similar concept has been proposed for Australia and Asia.

Results and discussion

Changes in PV and CSP energy output

The change in calculated PV and CSP energy outputs are presented as both time series covering selected regions and as global maps, all using a baseline of the 1980–1999 mean. Fig. 1 presents a series of maps showing the absolute change in temperature and insolation (total and direct), and the percentage change in PV
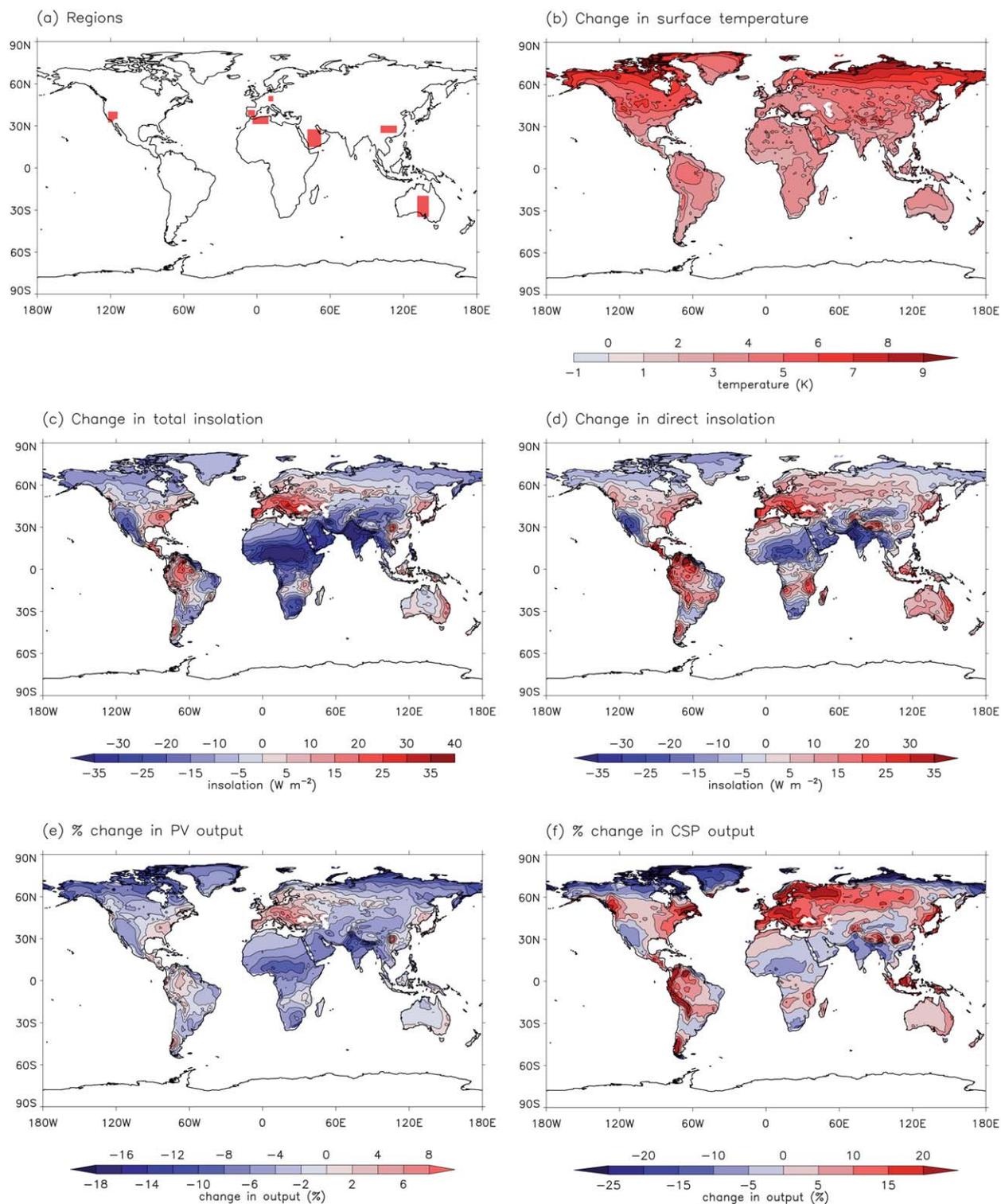
Fig. 1 (a) Global map identifying the regions included in the PV and CSP trends shown in Fig. 2–5. Global maps showing the change to 2080 in (b) daytime temperature, (c) daytime total insolation, (d) daytime direct insolation, (e) percentage change in PV output, and (f) percentage change in CSP output. Data is from the HadGEM1 model simulation.

and CSP output, all over a 10-year mean centred on 2080. Only data from the HadGEM1 model is presented. Maps generated from the HadCM3 model data show similar features. Major differences are discussed later in this section.

Fig. 2 and 3 present plots of percentage change in respectively PV and CSP output. Each region is considered separately, and data from both models is included. Note that different plots have different ranges for the *y*-axis. While there is year-to-year

3104 | *Energy Environ. Sci.*, 2011, **4**, 3101–3109

This journal is © The Royal Society of Chemistry 2011

Table 1 Regions included in the calculations

Region	Location	Selected large solar power plants (2010)
California	238°– 242° E, 32°– 40° N	Topaz solar farm (550 MW, PV, in development)
		SEGS I–VII (354 MW total, CSP, operational)
Nevada	242°– 246° E, 35°– 40° N	Copper Mountain (48 MW, PV, operational)
		Nevada Solar One (64 MW, CSP, operational)
Spain	352°– 360° E, 37°– 42° N	Olmedilla de Alarcon (60 MW, PV, operational)
		Solnova I–V (250 MW total, CSP, operational)
Algeria (north)	356°– 10° E, 31°– 37° N	Part of Desertec (EU-MENA) (CSP, concept)
Germany (south)	9°– 14° E, 47°– 52° N	Finsterwalde (80 MW, PV, operational)
		Straßkirchen (54 MW, PV, operational)
Saudi Arabia	41°– 53° E, 15°– 28° N	Part of Desertec (EU-MENA) (CSP, concept)
China (south)	100°– 115° E, 24°– 30° N	Kunming (166 MW, PV, partly operational)
Australia (south)	130°– 142° E, 20°– 35° S	Part of Desertec (CSP, concept)
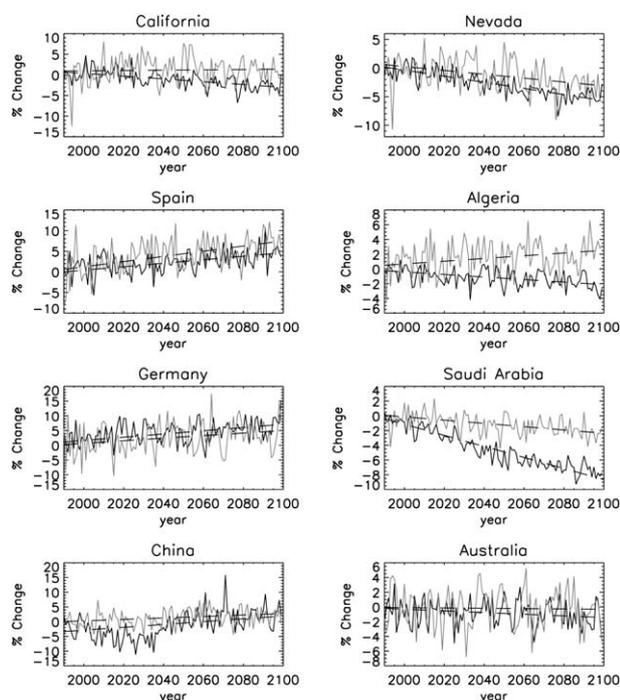
Fig. 2 Plots of percentage change in PV output for different regions for both models (HadGEM1 in black, HadCM3 in grey). The dashed line shows the best-fit linear trend.

variability, all long-term trends are clearly linear, so a best-fit straight line is included for each plot. The only exception is PV output in China for the HadGEM1 model which shows a distinct decrease to 2020 followed by an increase. In developing nations, such as China, sulphur emissions in the SRES A1B scenario rise to a peak at 2020 and then decline because of the expected introduction of clean air acts to control emissions. Total insolation in China for the HadGEM1 model decreases to 2020 and then increases (not shown). This is likely to be caused by sulphate aerosols and their effects on cloud properties, although it is not clear why the direct insolation does not show such a clear pattern. The HadCM3 model does not show this pattern because of its less physical realisation of aerosols. Sulphur emissions decrease slowly over the 21st century in North America and Europe where clean air acts have already imposed controls.

Fig. 4 shows percentage changes in PV and CSP output from 2010 to 2080 calculated from best-fit straight lines of the absolute output. It is clear that there are considerable regional differences. Conclusions are drawn mainly from the HadGEM1 model which is superior in its aerosol representation, but HadCM3 results are included to illustrate model projection differences. PV output is likely to increase by a few percent in Europe and China, see little change in Algeria and Australia, and decrease by a few percent in western USA and Saudi Arabia. CSP output is likely to increase by more than 10% in Europe, increase by several percent in China and a few percent in Algeria and Australia, and decrease by a few percent in western USA and Saudi Arabia. However, the lower absolute G_{dir} in Germany may still make PV the more economic choice. Uncertainties in outputs for these locations and for other locations with notable change, consistent between models, are considered later.

Temperature and insolation contributions

It is informative to attribute changes in PV and CSP output to changes in T and G (G_{tot} for PV and G_{dir} for CSP). Equations for ΔP_{PV} and ΔP_{CSP} in terms of ΔT, ΔG, and ΔG^2 are derived from eqn (4), (5), (7), and (8) as

$$
\begin{aligned}
\frac{\Delta P_{PV}}{\eta_{ref}} = & -\Delta T G_{tot} \beta c_2 \\
& + \Delta G_{tot}\left(1 - \beta c_1 + \beta T_{ref} - 2\beta c_3 - T\beta c_2\right) \\
& - \Delta G_{tot}^2 \beta c_3 - \Delta G_{tot}\Delta T \beta c_2 \\
& + \Delta G_{tot}\gamma \log_{10}(G_{tot} + \Delta G_{tot}) \\
& + G_{tot}\gamma \log_{10}\left(\frac{G_{tot} + \Delta G_{tot}}{G_{tot}}\right)
\end{aligned} \quad (10)
$$

and

$$
\Delta P_{CSP} = \Delta T k_1 + \Delta G_{dir} k_0 \quad (11)
$$

To calculate the relative contributions from ΔT and ΔG, ΔE_{PV} and ΔE_{CSP} were calculated with respectively either G or T held constant at their 1980–1999 mean so either $\Delta G = 0$ or $\Delta T = 0$. The results of this calculation for different regions, technologies, and models are shown in Fig. 5 where each pair of bars show the fractional contribution from respectively ΔT and ΔG, calculated from linear trends. The sum of the two fractions is close to 1, with
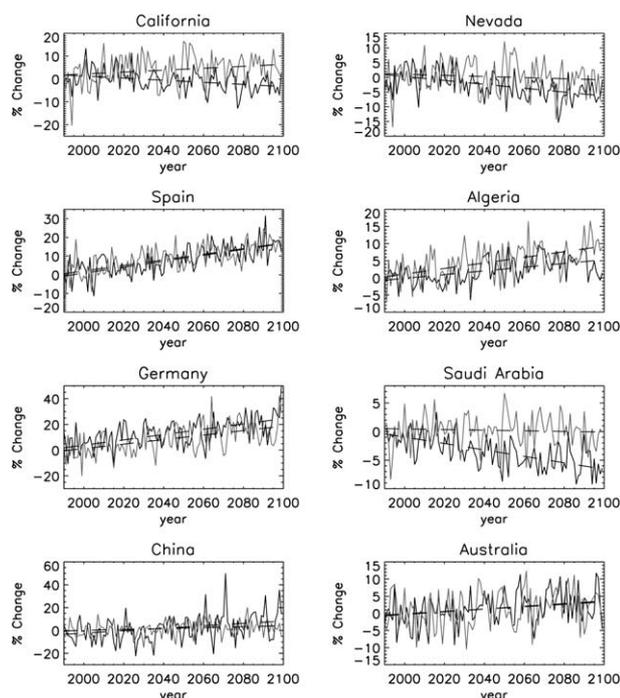
Fig. 3 Plots of percentage change in CSP output for different regions for both models (HadGEM1 in black, HadCM3 in grey). The dashed line shows the best-fit linear trend.

small deviations caused by cross products. Fractions less than 0 and greater than 1 indicate that ΔT and ΔG are driving the output in opposite directions.

For PV, fractional contributions are strongly dependent on the region. There are a few cases where output changes caused by ΔT and ΔG compensate for each other resulting in an overall small change in output but large fractional contributions, such as PV from HadCM3 in California, Algeria, and Australia. For both models, in Spain, Germany, and China, an increase in T causes a decrease in E_{PV}, but this is outweighed by an increase in G, resulting in an overall large increase in E_{PV}. In Nevada and Saudi Arabia E_{PV} decreases because of an increase in T and decrease in G, with roughly equal model-average contributions. For CSP, fractional changes are less dependent on the region with a dominant contribution from changes in G in all cases. The compensation between ΔG and ΔT contributing to PV output and the dominant dependence on ΔG for CSP output accounts for the greater sensitivity to climate change often seen for CSP compared to PV. In some regions, such as Europe and Algeria, the direct insolation increases more than total insolation, which further increases CSP output compared to PV output.

Uncertainty in projected energy output

The uncertainty in future energy output originating from the uncertainty in temperature change is calculated from projected temperature changes in the regions of interest from the CMIP3 models. The difference between the upper and lower regional temperature changes, from different models, are very similar[23] and similar to that of the global mean. For HadGEM1 the global mean temperature change by 2100 is 1.7 °C above the lowest estimate and 1.0 °C below the highest estimate. Therefore,

calculations used the HadGEM1 insolation data and its temperature data plus (minus) a homogenously linearly scaled amount of up to 1.0 (1.7) °C higher (lower) by 2100. Similar calculations were performed for HadCM3 but using different upper and lower estimates as HadCM3 has a lower global mean temperature change. Estimates of changes in DTR are no more than 0.3 °C, and the uncertainty in minimum and maximum temperature is of the order of 0.5 °C.[12] The effect of uncertainty in DTR change on daytime temperature change would therefore be of the order of 0.2 °C, which is considerably smaller than the uncertainty in the change in temperature. The percentage changes in PV and CSP output from 2010 to 2080 for the temperature change minus and plus the scaled amount are shown as errors bars in Fig. 4. Inconsistencies between models beyond these error bars are caused by differences in projected insolation change.

Given that change in CSP output is dominated by change in insolation rather than temperature, it is not surprising that the CSP output range due to temperature change uncertainty is very small. The temperature change uncertainty for PV is typically 0.9%, but this is insufficient to alter the conclusions of this work.

To our knowledge, an analysis of differences in insolation changes over the 21st century between climate models that gives likely ranges in different regions does not exist. Therefore, it has not been possible to perform a similar estimate of uncertainty for insolation changes. However, Trenberth and Fasullo[24] assess changes in cloud amount and absorbed solar radiation (ASR) over the 20th and 21st centuries in 13 of the CMIP3 climate models which can provide some qualitative estimate of uncertainty in insolation, but note that it is not just cloud amount that defines insolation. Models disagree about cloud amount and ASR changes, even in the sign in some regions. However, there is good agreement of strong decreases in cloud and increases in ASR in southern Europe, suggesting our results for Europe are likely to be robust in all models. There is also good agreement of decreases in cloud and increases in ASR in Australia, much of Saudi Arabia and parts of China. In California and Nevada less than $3/4$ of the models agree in sign for cloud changes, with the mean being a small decrease, although there is better agreement in ASR. We found HadGEM1 and HadCM3 are inconsistent in California and Saudi Arabia, suggesting a higher uncertainty associated with these regions. Both models show areas of increasing CSP output in north-west USA and decreasing output in south-west USA. California lies near the interface of these areas so output is sensitive to the exact location of the interface which is model dependent.

With reference to Fig. 1(e) and 1(f), there are a few other regions in the world where notable energy output change is likely to occur. The eastern USA, countries in northern South America, and south-east Asian islands are likely to see a significant increase in CSP output. This was the case for both HadGEM1 and HadCM3, and there is good agreement between 13 models of strong cloud amount decreases in these regions and strong ASR increases in northern South America. Increase in CSP output was found in some regions of southern Africa for both HadGEM1 and HadCM3, and there is also good agreement between 13 models of strong cloud amount decreases and ASR increases here. Although a significant decrease in PV output was found in both HadGEM1 and HadCM3 in India, and neighbouring
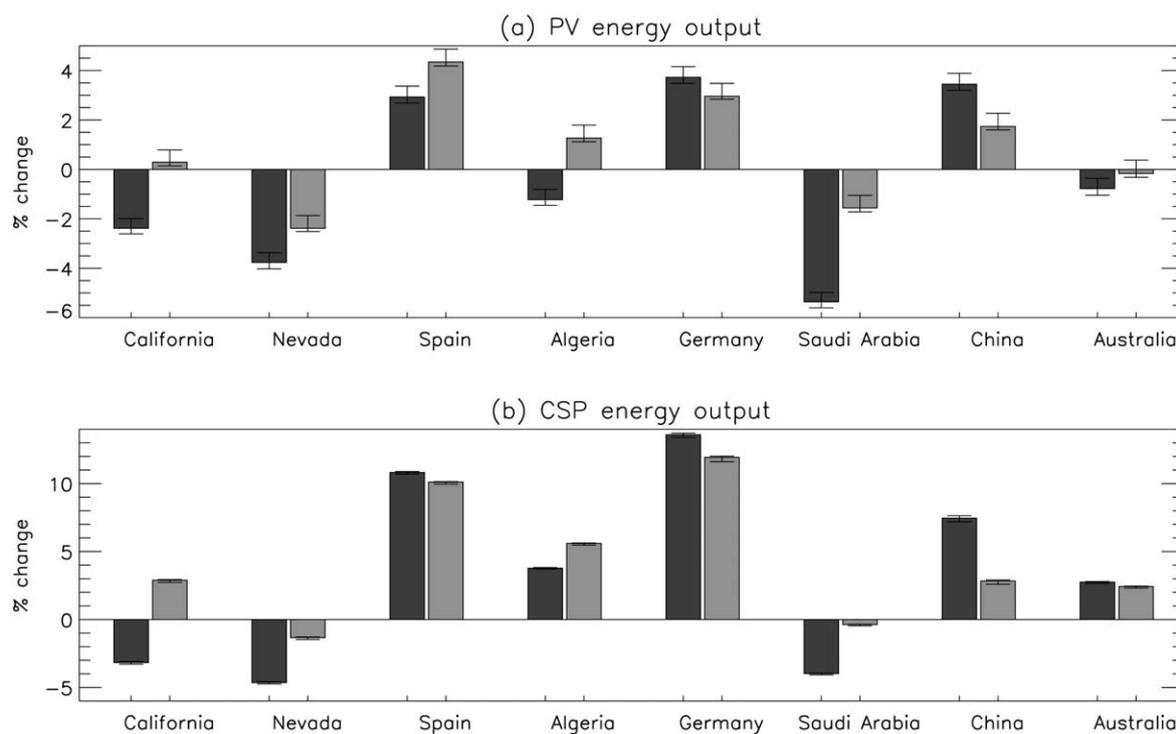
Fig. 4 Percentage change in energy output for PV and CSP for different regions for both models (HadGEM1 in dark grey, HadCM3 in light grey). Vertical error bars show the uncertainty due to temperature changes.

countries, and some central African countries, there is poor agreement between the 13 models in cloud amount in these regions.

Other PV technologies

Over the 21st century continued research and development may lead to an increased, or a dominant, market share for technologies other than crystalline silicon such as thin film PV (amorphous silicon, CdTe, CIGS), organic PV, dye sensitised PV, and multijunction concentrating PV. Each technology exhibits a different response to temperature and irradiance as shown in Table 2. The coefficients are indicative only and vary significantly depending on details of the device material and design. It must be noted that if PV is deployed on the massive scale implied by this work then some of these technologies face additional engineering challenges associated with degradation and scalability.

With the exception of dye sensitised PV and organic PV, the small irradiance coefficients have a negligible effect on change in energy output. For dye sensitised PV the temperature and irradiance coefficients are relatively large and negative, indicating that this technology will perform comparatively poorly in regions where insolation increases. In contrast, for organic PV both coefficients are large and positive, indicating it is notably robust to climate change in the same regions. Crystalline silicon has the most negative temperature coefficients making it relatively sensitive to climate change in locations expecting a large temperature rise. A more detailed comparison of the various technologies, including spectral and low-light response, is beyond the scope of this article but is highlighted as a topic that would benefit from future investigation.

Conclusions

Changes in PV output and its fractional contributions from temperature and insolation are all very location dependent. Our calculations suggest that PV output is likely to increase by a few percent in Europe and China, see little change in Algeria and Australia, and decrease by a few percent in western USA and Saudi Arabia. Change in CSP output is almost entirely caused by change in direct insolation. CSP output is likely to increase by more than 10% in Europe, increase by several percent in China and a few percent in Algeria and Australia, and decrease by a few percent in western USA and Saudi Arabia. This demonstrates that CSP is usually more sensitive to climate change than PV, although there are strong regional differences. These results are robust to uncertainty in projected temperature change, whereas a simple analysis of uncertainty in projected insolation change suggests strongest confidence in results for Europe and least confidence in results for western USA. It is clear from the linear nature of the changes in output in Fig. 2 and 3 that differences between models (uncertainties) become greater with time.

Changes in solar power plant output should be taken into account when selecting locations and technology for the new large-scale interconnected plants necessary to complete our transition to a low-carbon economy. A similar analysis using more climate models would give a better understanding of the uncertainty in energy output caused by uncertainty in projected insolation change, so these first results can be considered as an order of magnitude guide.

A number of other climatic variables have a notable impact on PV output. Wind influences the output of PV because forced convection removes heat from the cell and therefore reduces the
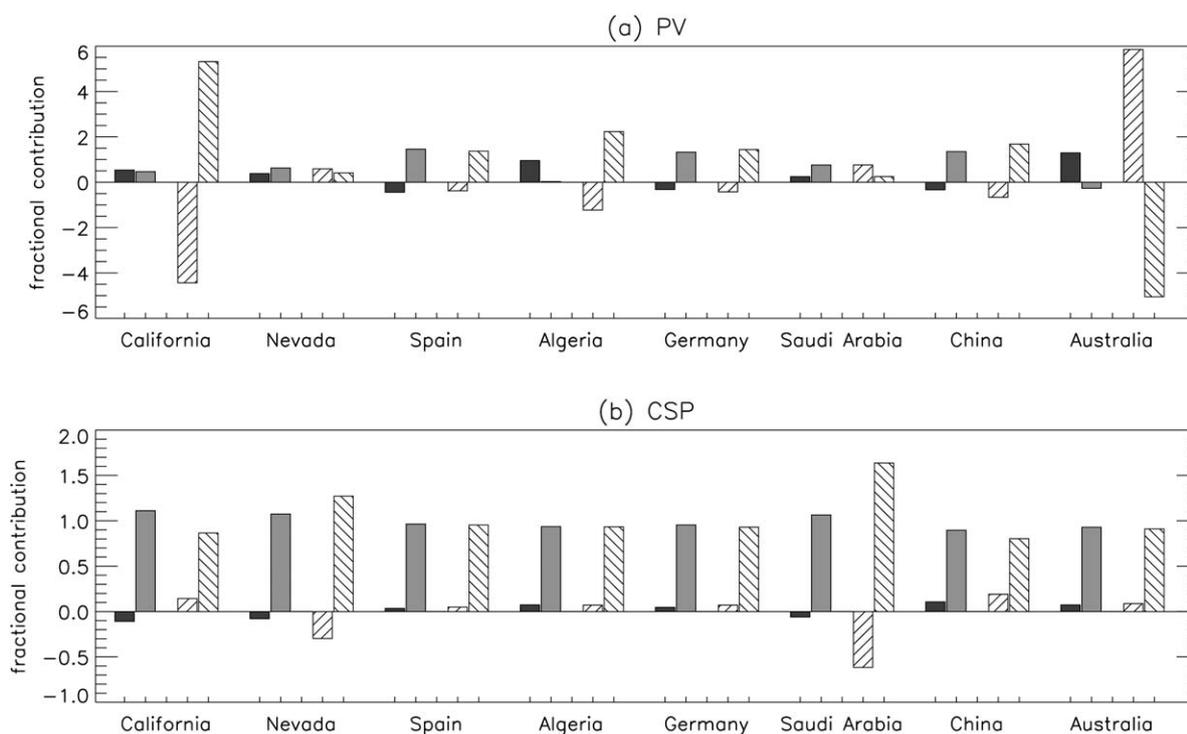
Fig. 5 Temperature (first bar of pair) and insolation (second bar of pair) fractional contributions to change in PV and CSP output for different regions for both models (HadGEM1 in solid bars, HadCM3 in striped bars).

Table 2 Typical temperature and irradiance coefficients for the efficiency of different PV technologies. Where the cell exhibits a non-linear response coefficients are taken for $T_{cell} = 40\,^{\circ}C$ and $G = 800$ W m^{-2}

Technology	Temperature coefficient ($\times\,10^{-3}$ K^{-1})	Irradiance coefficient ($\times\,10^{-3}$ W^{-1} m^2)
Monocrystalline silicon[15,16]	−4.5	0.05
Multicrystalline silicon[15,16,25]	−4	0.08
Amorphous silicon[15,16,25]	−2	−0.06
CdTe[15,16,26]	−2.5	−0.04
CIGS[15,16,25]	−3.5	−0.08
Organic[27,28]	4	0.5
Dye sensitised[29]	−4	−0.25
Multijunction concentrating[30–32]	−1.5	−0.035

cell temperature. Dust settling on PV panels and solar collectors is a significant problem in more arid regions, while rainfall cleans the panels removing dust. Large hail stones, while infrequent, have potential to shatter PV panels and solar collectors. These climate impacts deserve further investigation.

References

1 B. Parida, S. Iniyan and R. Goic, *Renewable Sustainable Energy Rev.*, 2011, **15**, 1625–1636.
2 S. A. Kalogirou, *Prog. Energy Combust. Sci.*, 2004, **30**, 231–295.
3 G. M. Martin, M. A. Ringer, V. D. Pope, A. Jones, C. Dearden and T. J. Hinton, *J. Clim.*, 2006, **19**(7), 1274–1301.
4 T. C. Johns, J. M. Gregory, W. J. Ingram, C. E. Johnson, A. Jones, J. A. Lowe, J. F. B. Mitchell, D. L. Roberts, B. M. H. Sexton, D. S. Stevenson, S. F. B. Tett and M. J. Woodage, *Climate. Dyn.*, 2003, **20**, 583–612.
5 G. A. Meehl, T. F. Stocker, W. D. Collins, P. Friedlingstein, A. T. Gaye, J. M. Gregory, A. Kitoh, R. Knutti, J. M. Murphy, A. Noda, S. C. B. Raper, I. G. Watterson, A. J. Weaver and Z.-C. Zhao, in *Climate Change 2007: The Physical Science Basis. Contribution of Working Group I to the Fourth Assessment Report of the Intergovernmental Panel on Climate Change*, ed. S. Solomon, D. Qin, M. Manning, Z. Chen, M. Marquis, K. B. Averyt, M. Tignor and H. L. Miller, Cambridge University Press, Cambridge, United Kingdom and New York, NY, USA, 2007, Ch. 10, pp. 749–845.
6 S. M. Uppala, P. W. KÅllberg, A. J. Simmons, U. Andrae, V. Da Costa Bechtold, M. Fiorino, J. K. Gibson, J. Haseler,

3108 | *Energy Environ. Sci.*, 2011, **4**, 3101–3109

This journal is © The Royal Society of Chemistry 2011

A. Hernandez, G. A. Kelly, X. Li, K. Onogi, S. Saarinen, N. Sokka, R. P. Allan, E. Andersson, K. Arpe, M. A. Balmaseda, A. C. M. Beljaars, L. Van De Berg, J. Bidlot, N. Bormann, S. Caires, F. Chevallier, A. Dethof, M. Dragosavac, M. Fisher, M. Fuentes, S. Hagemann, E. Hólm, B. J. Hoskins, L. Isaksen, P. A. E. M. Janssen, R. Jenne, A. P. Mcnally, J.-F. Mahfouf, J.-J. Morcrette, N. A. Rayner, R. W. Saunders, P. Simon, A. Sterl, K. E. Trenberth, A. Untch, D. Vasiljevic, P. Viterbo and J. Woollen, *Q. J. R. Meteorol. Soc.*, 2005, **131**, 2961–3012.

7 M. Wild, C. N. Long and A. Ohmura, *J. Geophys. Res.*, 2006, **111**, D01104, DOI: 10.1029/2005JD006118.

8 A. Bodas-Salcedo, M. A. Ringer and A. Jones, *J. Clim.*, 2008, **21**(18), 4723–4748.

9 J. M. Edwards and A. Slingo, *Q. J. R. Meteorol. Soc.*, 1996, **122**, 689–720.

10 *Special Report on Emissions Scenarios. A Special Report of Working Group III of the Intergovernmental Panel on Climate Change*, ed. N. Nakićenović and R Swart, Cambridge University Press, 2000.

11 P. Brohan, J. J. Kennedy, I. Harris, S. F. B. Tett and P. D. Jones, *J. Geophys. Res.*, 2006, **111**, D12106, DOI: 10.1029/2005JD006548.

12 D. B. Lobell, C. Bonfils and P. B. Duffy, *Geophys. Res. Lett.*, 2007, **34**, L05715, DOI: 10.1029/2006GL028726.

13 M. D. Archer and R. Hill (ed.), *Clean electricity from photovoltaics*, 2001, Imperial College Press, London.

14 E. Skoplaki and J. A. Palyvos, *Sol. Energy*, 2009, **83**, 614–624.

15 H. A. Zondag, *Renewable Sustainable Energy Rev.*, 2008, **12**, 891–959.

16 D. L. Evans, *Sol. Energy*, 1981, **27**, 555–560.

17 Q. Kou, S. A. Klein and W. A. Beckman, *Sol. Energy*, 1998, **64**, 33–40.

18 J. A. Duffie and W. A. Beckman, *Solar Energy Thermal Processes*, third ed., 2006, Wiley, Hoboken, NJ, §23.3.

19 F. Lasiner and T. G. Ang, *Photovoltaic Engineering Handbook*, 1990, Adam Higler, Princeton.

20 J. A. Duffie, W. A. Beckman, *Solar engineering of thermal processes*, 1991, Wiley, New York.

21 V. Dudley, *SANDIA Report test results for industrial solar technology parabolic trough solar collector*. SAND-94-1117, Albuquerque, USA: Sandia National Laboratory; 1995.

22 *The Desertec concept for energy, water, and climate security white book*, 4th edition. Bonn, Desertec Foundation.

23 J. H. Christensen, B. Hewitson, A. Busuioc, A. Chen, X. Gao, I. Held, R. Jones, R. K. Kolli, W.-T. Kwon, R. Laprise, V. Magaña Rueda, L. Mearns, C. G. Menéndez, J. Räisänen, A. Rinke, A. Sarr and P. Whetton, in *Climate Change 2007: The Physical Science Basis. Contribution of Working Group I to the Fourth Assessment Report of the Intergovernmental Panel on Climate Change*, ed. S. Solomon, D. Qin, M. Manning, Z. Chen, M. Marquis, K. B. Averyt, M. Tignor and H. L. Miller, Cambridge University Press, Cambridge, United Kingdom and New York, NY, USA, 2007, Ch. 11, pp.848–940.

24 K. E. Trenberth and J. T. Fasullo, *Geophys. Res. Lett.*, 2009, **36**, L07706, DOI: 10.1029/2009GL037527.

25 N. H. Reich, S. Y. Kan, W. G. J. H. M. van Sark, E. A. Alsema, S. Silvester, A. S. H. van der Heide, R. W. Lof and R. E. I. Schropp, *Weak light performance and spectral response of different solar cell types, Proceedings of the 20th European Photovoltaic Solar Energy Conference and Exhibition Barcelona*, Spain, 2005.

26 J. A. del Cueto, *Progr. Photovolt.: Res. Appl.*, 1998, **6**, 433–446.

27 M. R. Mitroi1, V. Iancu1, L. Fara1 and M. L. Ciurea, *Prog. Photovoltaics*, 2011, **19**, 301–306.

28 E. A. Katz, D. Faiman, S. M. Tuladhar, J. M. Kroon, M. M. Wienk, T. Fromherz, F. Padinger, C. J. Brabec and N. S. Sariciftci, *J. Appl. Phys.*, 2001, **90**, 5343–5350.

29 M. Berginc, U. O. Krašovec, M. Jankovec and M. Topic, *Sol. Energy Mater. Sol. Cells*, 2007, **91**, 821–828.

30 R. R. King, D. C. Law, K. M. Edmondson, C. M. Fetzer, G. S. Kinsey, H. Yoon, R. A. Sherif and N. H. Karam, *Appl. Phys. Lett.*, 2007, **90**, 183516.

31 G. S. Kinsey, P. Pien, P. Hebert and R. A. Sherif, *Sol. Energy Mater. Sol. Cells*, 2009, **93**, 950–951.

32 P. J. Verlinden, A. Lewandowski, H. Kendall, S. Carter, K. Cheah, I. Varfolomeev, D. Watts, M. Volk, I. Thomas, P. Wakeman, A. Neumann, P. Gizinski, D. Modra, D. Turner and J. B. Lasich, *PVSC: 33rd IEEE Photovoltaic specialists conference*, 2008, 1552–1557.